Inferring thermodynamic properties from CCN activation experiments: a) single-component and binary aerosols

L. T. Padró, A. Asa-Awuku, R. Morrison, A. Nenes

Atmos. Chem. Phys. Discuss., 7, 3805–3836, 2007
www.atmos-chem-phys-discuss.net/7/3805/2007/

Atmospheric Chemistry and Physics Discussions

Inferring thermodynamic properties from CCN activation experiments: a) single-component and binary aerosols

L. T. Padró[1], A. Asa-Awuku[1], R. Morrison[1,*], and A. Nenes[1,2]

[1]School of Chemical and Biomolecular Engineering, Georgia Institute of Technology, Atlanta, GA, 30332, USA
[2]School of Earth and Atmospheric Sciences, Georgia Institute of Technology Atlanta, GA, 30332, USA
[*]now at: Department of Chemical Engineering, University of Texas, Austin, TX, 78712, USA

Received: 12 February 2007 – Accepted: 2 March 2007 – Published: 15 March 2007

Correspondence to: A. Nenes (nenes@eas.gatech.edu)

Abstract

This study presents a new method, Köhler Theory Analysis (KTA), to infer the molar volume and solubility of organic aerosol constituents. The method is based on measurements of surface tension, chemical composition, and CCN activity coupled with Köhler theory. KTA is evaluated by inferring the molar volume of six known organics (four dicarboxylic acids, one amino acid, and one sugar) in pure form and in mixtures with ammonium sulfate ($(NH_4)_2SO_4$). Inferred molar volumes are to within 18% of their expected value for organic fractions between 90 and 100%. This suggests that KTA is a powerful and ideal method for determining the CCN characteristic of ambient water soluble organic carbon (WSOC) and provide physically-based constraints for aerosol-cloud interaction parameterizations.

1 Introduction

It is well accepted that atmospheric aerosols affect climate directly by reflecting incoming solar radiation (IPCC, 2001) and indirectly through their role as cloud condensation nuclei (CCN) (Twomey, 1977; Albrecht, 1989; IPCC, 2001). Understanding the cloud droplet formation potential of aerosols is a requirement for predicting their impacts on clouds, and currently consists of a large source of uncertainty in climate change predictions. Aerosols in the atmosphere are composed of inorganic and organic compounds which influence the particle ability to form CCN. Past studies have shown that particulate matter composed of water soluble inorganic salts and low molecular weight dicarboxylic organic acids can act as efficient CCN (Cruz and Pandis, 1997; Facchini et al., 1999a; Giebl et al., 2002; Raymond and Pandis, 2002; Kumar et al., 2003) which is adequately modeled by Köhler theory (Kohler, 1936). Although less accurate, Köhler theory can still predict, with appropriate modifications (primarily to relax the assumption of limited solubility), the CCN activity of higher molecular weight organic compounds such as some dicarboxylic acids, fatty acids, alcohols, and amines (Raymond and Pan-

dis, 2002; Hartz et al., 2006) which constitute a significant fraction of the water soluble species (Zappoli et al., 1999; Decesari et al., 2000; Broekhuizen et al., 2005; Sullivan and Weber, 2006a; Sullivan and Weber, 2006b).

Organics primarily influence CCN activity by contributing solute and depressing surface tension; both affecting the equilibrium water vapor pressure needed for droplet activation (Shulman et al., 1996; Facchini et al., 1999b; IPCC, 2001; Feingold and Chuang, 2002; Nenes et al., 2002; Kanakidou et al., 2005). A modified version of Köhler theory incorporating both limited solute solubility and surface tension depression for slightly soluble species was first presented by Shulman et al. (1996); subsequently, Facchini et al. (2000) showed that the surface tension depression could be important for water soluble organic carbon (WSOC) typically found in polluted environments. Decesari et al. (2000) found that WSOC is composed of a complex mixture of neutral and acidic polar compounds, the most hydrophobic of which are responsible for the surface tension depression. Organics may also impact the droplet growth kinetics of CCN (Feingold and Chuang, 2002; Nenes et al., 2002), but is currently not the subject of this study.

Apart from surface tension depression, the solute thermodynamic properties such as the molar volume (molar mass over density), solubility, and effective van't Hoff factor affect CCN activity. Such parameters are very difficult to determine for ambient aerosols, as they are a complex and highly variable mixture of organic/inorganic compounds. As challenging as it may be, this characterization is required to establish a physically-based link between organic aerosol and cloud droplet formation. In this work, we propose and develop a new methodology called Köhler Theory Analysis (KTA) to address this need. KTA is based on using Köhler theory to infer molar volume and solubility from CCN activation measurements (measurements of chemical composition and surface tension may be required as well). In subsequent sections, we present the theoretical basis of KTA and its application. KTA is then evaluated by inferring the molar volume of six known organics (four dicarboxylic acids, one amino acid, and one sugar) in pure form and in mixtures with $(NH_4)_2SO_4$.

2 Köhler theory analysis

2.1 Single component CCN

Köhler theory is based on thermodynamic equilibrium arguments and computes the equilibrium saturation ratio, S, of a wet particle of diameter, D_p, from the contribution of curvature (Kelvin) and solute (Raoult) terms,

$$S = \frac{P^w}{P^{sat}_{flat,w}} = \exp\left(\frac{A}{D_p} - \frac{\upsilon\phi n_s}{n_w}\right) \quad (1)$$

where $A = \frac{4M_w\sigma}{RT\rho_w}$, P^w is the droplet water vapor pressure, $P^{\text{sat}}_{\text{flat},w}$ is the saturation water vapor pressure over a flat surface at the temperature T, M_w is the molar mass of water, σ is the droplet surface tension at the point of activation, R is the ideal gas constant, ρ_w is the density of water, υ is the effective van't Hoff factor of the solute, ϕ is the osmotic coefficient, n_s is the moles of solute, and n_w is the moles of water. The Kelvin or curvature effect (A term) is dependent on the droplet surface tension and tends to increase the saturation ratio while the Raoult's or solute effect tends to decrease the saturation ratio by contribution of solute to the growing droplet.

If the CCN is composed of a single component that completely dissolves in water and is diluted (ϕ=1) in the drop, Eq. (1) reduces to (Seinfeld and Pandis, 1997),

$$\frac{P^w}{P^{\text{sat}}_{\text{flat},w}} = \exp\left(\frac{A}{D_p} - \frac{B}{D_p^3}\right) \quad (2)$$

where:

$$B = \frac{6n_sM_w\upsilon}{\pi\rho_w} \quad (3)$$

ACPD
7, 3805–3836, 2007

EGU

and the maximum ("critical") saturation ratio of the Köhler curve is given by,

$$S_c = \exp\left(\frac{4A^3}{27B}\right)^{1/2} \quad (4)$$

S_c corresponds to the minimum level of water vapor saturation required for a CCN to develop into a cloud droplet. Since critical saturations are always higher than unity, the critical supersaturation, s_c (defined as S_c-1) is often used in its place. For each s_c, there is a characteristic dry diameter (d_{pc}), above which all particles activate into cloud droplets.

2.2 Multi-component CCN

If the aerosol is composed of more than one component (e.g., organic and inorganic), Köhler theory can still be applied with appropriate modifications to the Raoult's (solute) term:

$$B = \sum_i B_i = \sum_i \left(\frac{\rho_i}{\rho_w}\right)\left(\frac{M_w}{M_i}\right)\varepsilon_i \upsilon_i d^3 = d^3\left(\frac{M_w}{\rho_w}\right)\sum_i \left(\frac{\rho_i}{M_i}\right)\varepsilon_i \upsilon_i \quad (5)$$

where d is the dry diameter of the CCN, and ρ_i, ε_i, υ_i, and M_i are the density, volume fraction, effective van't Hoff factor and molar mass of the solute i, respectively. ε_i is related to the mass fraction of i, m_i, as:

$$\varepsilon_i = \frac{m_i/\rho_i}{\sum_i m_i/\rho_i} \quad (6)$$

where m_i is assumed to be known from measurements. For a single component aerosol ε_i=1 which reduces Eq. (5) to Eq. (3).

2.3 Köhler theory analysis: inferring molar volume

If the CCN is a mixture of completely soluble organic and inorganic material then theory gives,

$$s_c = \left(\frac{256M_w^3\sigma^3}{27R^3T^3\rho_w^3}\right)^{1/2}\left[\sum_i\left(\frac{\rho_w}{M_w}\right)\left(\frac{M_i}{\rho_i}\right)\frac{1}{\varepsilon_i\upsilon_i}\right]^{1/2} d^{-3/2} = \omega d^{-3/2} \quad (7)$$

where

$$\omega = \left(\frac{256M_w^3\sigma^3}{27R^3T^3\rho_w^3}\right)^{1/2}\left[\sum_i\left(\frac{\rho_w}{M_w}\right)\left(\frac{M_i}{\rho_i}\right)\frac{1}{\varepsilon_i\upsilon_i}\right]^{1/2} \quad (8)$$

If ω is known from CCN activity measurements, the molar volume of the water soluble organic component (WSOC), $\frac{M_j}{\rho_j}$, can be inferred if the surface tension at the point of activation, organic and inorganic fraction as well as the effective van't Hoff factor of the components present (which a value of ~1 for organics and ~2.5 for $(NH_4)_2SO_4$ was used) are known. $\frac{M_j}{\rho_j}$ can be explicitly solved by rearranging Eq. (8) as follows:

$$\frac{M_j}{\rho_j} = \frac{\varepsilon_j\upsilon_j}{\frac{256}{27}\left(\frac{M_w}{\rho_w}\right)^2\left(\frac{1}{RT}\right)^3\sigma^3\omega^{-2} - \sum_{i\neq j}\frac{\rho_i}{M_i}\varepsilon_i\upsilon_i} \quad (9)$$

where j is used to denote the organic component of the aerosol and i refers to all compounds (organic, inorganic, except "j") present in the particle.

Equation (9) is the basis of Köhler Theory Analysis (KTA), and can be applied as follows:

a. If there are no strong surfactants present (i.e., surface tension of the CCN at the point of activation does not depend on the solute concentration), ω does not

depend on d and its value can be determined by a power law fit to the CCN activation curves. Equation (9) is then applied to infer the WSOC molar volume, given that the volume fractions and composition of organics and inorganic presents are known. This method is applied primarily in this study.

b. If there are strong surfactants present (i.e., surface tension of the CCN at the point of activation is strongly dependant on the solute concentration), ω depends on d therefore the WSOC molar volume has to be solved for each supersaturation by incorporating the surface tension depression at each d. ω is still determined by a power law fit to the CCN activation curves what changes is how Eq. (9) is applied to the data. Two methods can be used:

   b_1. Since the CCN is dilute at the point of activation at low supersaturations (i.e., ω does not depend on d since there are no strong surfactants present) method "a" can be applied for this range. The appropriate supersaturation range can be determined by examining the slope (d exponent) of the activation curves.

   b_2. When the CCN can not be assumed to be dilute at the point of activation (high supersaturations), the WSOC molar volume is inferred at each supersaturation due to changes in the surface tension with d. We then compute the average molar volume over the range of supersaturations considered.

2.4 Molar volume uncertainty analysis

The uncertainty in inferred organic molar volume, $\Delta\left(\frac{M_j}{\rho_j}\right)$, is estimated as

$$\Delta\left(\frac{M_j}{\rho_j}\right) = \sqrt{\sum_{\text{for all } x} \left(\Phi_x \Delta x\right)^2} \tag{10}$$

where Φ_x is the sensitivity of molar volume to each of the measured parameters x (i.e., any of σ, ω, and υ_j)

$$\Phi_x = \frac{\partial}{\partial x}\left(\frac{M_j}{\rho_j}\right) \tag{11}$$

and Δx is the uncertainty in x. The Φ_x for Eq. (10) is obtained by differentiating Eq. (9) and are shown in Table 1.

2.5 Köhler theory analysis: inferring solubility

From Eq. (7), s_c for completely soluble CCN scales with $d^{-3/2}$. However, if an aerosol exhibits limited solubility, s_c will change its scaling dependence at a characteristic dry diameter d^* (Fig. 1). This is because when $d<d^*$, the amount of water available at the point of activation is insufficient to dissolve all available solute (which gives a much steeper dependence of s_c vs. d). For $d>d^*$, all solute is dissolved and s_c scales with $d^{-3/2}$. Hence, $d=d^*$ corresponds to the solubility limit of the solute, which can be expressed as:

$$C_{eq} = \frac{27}{8}\varepsilon_j \rho_s \frac{d^{*3} s_c^{*3}}{A^3} \tag{12}$$

where s_c^* is the critical supersaturation of the particle with dry diameter d^*.

3 Experimental procedure

3.1 Surface tension measurements

Surface tension is measured using a pendant drop tensiometer (CAM 200 Optical Contact Angle Meter, by KSV Inc.). A mechanically-controlled micro-syringe slowly drops

the solution into a chamber where a snapshot of the droplet at the tip of a stainless steel needle is taken. Approximately seventy pictures (ten pictures per droplet) of seven different droplets (right before they fall off the tip) were taken in order to obtain averages and standard deviations for each solution. When taking the snapshots, it is desirable to obtain the maximum volume possible in the droplet without it falling since it gives a more accurate σ value. The droplet shape is then fit to the Young-Laplace equation (Spelt and Li, 1996) from which the sample surface tension is obtained. Carbon concentration was chosen as a basis for surfactant concentration (Facchini et al., 1999b). Surface tension depression depends on the amount of dissolved carbon; therefore it is measured over a range of concentrations, starting at near the bulk solubility limit and then 1:2, 1:4, 1:8 dilutions with ultrafine pure water. Finally, one more "pure water" measurement was done corresponding to a zero carbon concentration solution. A plot of the solution surface tension, σ, versus the water soluble organic carbon concentration (C_{WSOC}) was obtained for each inorganic/organic mixture and the data fitted to the Szyskowski-Langmuir equation (Langmuir, 1917),

$$\sigma = \sigma_w - \alpha T \ln(1 + \beta C_{\mathrm{WSOC}}) \tag{13}$$

where σ_w is the surface tension of water at temperature T and the parameters α and β are obtained by least squares minimization.

In order to apply the surface tension into KTA, the surface tension at the point of activation has to be calculated for each supersaturation. First we need to calculate the concentration of the organic present in the activated particle from the s_c and d data obtained from the CCN measurements. The average concentration of the organic at activation, C_{act}, is determined by:

$$C_{\mathrm{act}} = \frac{27}{8} \varepsilon_j \rho_s \frac{d^3 s_c^3}{A^3} \tag{14}$$

where ρ_s is the density of the aerosol particle. C_{act} is then substituted into Eq. (13) to obtain the surface tension at the point of activation.

3.2 CCN activity measurements

The setup used for measurement of CCN activity consists of three sections: aerosol generation, particle size selection, and CCN/CN measurement (Fig. 2). In the aerosol generation step, an aqueous solution of organic/inorganic is atomized with a controlled high velocity air stream atomizer. Compressed filtered air is introduced into the atomizer, the pressure of which controls the size distribution and flow rate of atomized droplets. A polydisperse aerosol is subsequently produced by drying the droplet stream by passing it through two silica-gel diffusion dryers.

The dry aerosol is then sent to the electrostatic classifier for particle size selection (ES TSI Model 3080) with a Differential Mobility Analyzer (DMA, TSI Model 3081). Before entering the classifier, the aerosols are passed through an impactor to remove supermicron particles; the remaining aerosol passes through a Kr-35 neutralizer which charges the particles. The particle size is then selected by a Differential Mobility Analyzer by allowing particles of the selected size (charge) to pass through producing a monodisperse aerosol. The monodisperse flow exiting the DMA at $1\,\mathrm{l\,min^{-1}}$ is mixed with filtered air and then sampled by a Condensation Particle Counter (CPC, TSI Model 3010), and a Cloud Condensation Nuclei (CCN, DMT Inc.) Counter.

The CPC measures the total number concentration of condensation nuclei (CN) present for the specified aerosol size while the CCN counts the total number of particles that become activated as the aerosol is exposed to a constant water supersaturation. The CCN instrument operates by applying a linear temperature gradient across a wetted column; water vapor diffuses more quickly than heat, resulting in a constant water supersaturation along a streamline (Roberts and Nenes, 2005). CCN flowing about the column centerline activate and grow into cloud droplets (D_p>1 μm) and are counted at the exit with an optical particle counter (OPC; 0.18W and 500 THz). For our studies, particles ranging between 7 and 325 nm dry mobility diameters were selected and exposed to 0.2%, 0.4%, 0.6% and 1.2% supersaturation (SS) to obtain CCN activation curves (Fig. 3). The CCN instrument is calibrated daily with $(NH_4)_2SO_4$ to verify that it

is operating properly.

Two approaches were applied to perform the particle size selection. In the first approach, called "stepping mode", the DMA voltage (i.e., monodisperse aerosol diameter) is constant for a period of time, during which the average CN and CCN concentrations are measured. This procedure is repeated over many particle sizes and CCN supersaturations. In the second approach, called Scanning Mobility CCN Analysis or SMCA (Nenes and Medina, 2007[1]), the DMA voltage is changed over time, so that the complete size range of dry particle size is "scanned" over 2 min. The time series of CN, CCN and voltage is then converted into activation curves using an inversion method (Nenes and Medina, 2007[1]). SMCA greatly reduces the time required for CCN activity measurements and the amount of sample required for its complete characterization.

CCN activity is characterized by the minimum dry particle diameter, d_{p50}, that activates at the supersaturation of interest. d_{p50} is found by plotting the ratio of CCN to CN concentration as a function of dry particle diameter and determining the dry diameter for which the CCN/CN ratio equals 0.50. To facilitate with the analysis, the data is fit to a sigmoid curve which then avoids considering the impact of multiply-charged particles (shown in Fig. 3 as a "hump" left to the sigmoid curve).

3.3 Compounds considered in this study

Table 2 summarizes the properties of seven compounds (one inorganic salt and seven organics) used in the experiments. Because of its atmospheric relevance, $(NH_4)_2SO_4$ was chosen as the inorganic salt. The organics include four carboxylic acids (succinic acid, azelaic acid, phthalic acid, and malonic acid), one amino acid (leucine), and one sugar (fructose). Succinic, azelaic, and malonic acids are dicarboxylic acids of varying chain length, while phthalic acid is a dicarboxylic acid with a benzene ring. Leucine is

[1] Nenes, A. and Medina, J.: Scanning Mobility CCN Analysis – A new method for fast measurements of size-resolved CCN activity and growth kinetics, Aerosol Sci. Tech., in review, 2007.

a branched six carbon amino acid with a carboxylic acid group and an amine group. Finally, fructose is a six carbon sugar that exists interchangeably between a chain and a 5-carbon ring structure. All of these compounds are representative of various biogenic and anthropogenic compounds found in atmospheric particles (Saxena and Hildemann, 1996), all with varying water solubility, carbon chain length and surfactant characteristics.

For each organic compound, we characterized the surfactant properties and CCN activity for organic-$(NH_4)_2SO_4$ mixtures with the following organic/inorganic molar ratios: 100:0, 99:1, 95:5, 90:10, 50:50, 10:90, and 1:99. By varying the organic mass fraction, we assess the applicability of KTA over a wide range of organic/inorganic interaction strength. This is a particularly important test, as it will largely determine its applicability for complex mixtures typical of atmospheric aerosols. Finally, we quantify the uncertainty of the inferred molar volume from uncertainties in σ, ω, υ_j for all mixtures considered.

4 Results

4.1 Surface tension measurements

Surface tension was measured for all pure organic and mixtures with $(NH_4)_2SO_4$ as a function of C_{WSOC}; the data was subsequently fit to the Szyskowski-Langmuir equation for use in KTA. Figure 4 shows the surface tension dependence of C_{WSOC} for all organic species (high organic fraction) each fitted to the Szyskowski-Langmuir equation. All compounds were found to depress surface tension except for phthalic acid in the range of concentration studied. The strongest surface active compounds were malonic acid and azelaic acid; fructose, leucine and succinic acid showed moderate surfactant behavior in the range of concentrations considered.

To address the effects of salts in the surfactant behavior of organics, we compared the surface tension depression of each organic when dissolved in water alone and

mixed with $(NH_4)_2SO_4$. Examples of the surface tension dependence of pure succinic acid and mixtures with $(NH_4)_2SO_4$ are shown in Fig. 5a (high organic fractions) and Fig. 5b (low organic fractions). Adding small amounts of $(NH_4)_2SO_4$does not affect the surfactant behavior of succinic acid at high organic fractions (Fig. 5a). On the other hand at low organic concentrations, introduction of greater amounts of $(NH_4)_2SO_4$ to the succinic acid solution can further decrease the surface tension beyond that of the pure organic (Fig. 5b). As an example for a C_{WSOC} of 2000 ppm, the surface tension for pure succinic acid (100%) is 71 mN m^{-1} while for a 1% succinic acid solution, at the same concentration, the surface tension is depressed down to 66.5 mN m^{-1}. The observed decrease in surface tension with increase in salt concentration could be explained by the interaction between ammonium sulfate and organics molecules. The presence of the inorganic electrolyte at high concentrations forces the organic to partition to the surface creating a surfactant rich layer; therefore, decreasing the surface tension beyond that of the pure organic component (Kiss et al., 2005).

Since the addition of $(NH_4)_2SO_4$ did not substantially affect the droplet surface tension for the high organic fraction solutions considered (90%–100%), all molar fraction solutions of each species were fit to Eq. (13) in order to obtain average α and β parameters (Table 3), which subsequently can be introduced to KTA. For low organic fractions (50%, 10%, and 1%) $(NH_4)_2SO_4$ has an important impact on surface tension, so α and β must be determined at each sulfate concentration (Table 4; Fig. 5b).

4.2 CCN measurements

Activation curves for pure succinic acid and mixtures with $(NH_4)_2SO_4$ are shown in Fig. 6. Our data shows that as the organic mass fraction decreases from 100% to 50%, the activation curves of the mixtures move towards the $(NH_4)_2SO_4$ curve. Therefore having small amounts of salt present is able to increase slightly the CCN activity of the organic in solution. On the other hand, when small amounts of organic are introduced in a highly concentrated $(NH_4)_2SO_4$ solution, the aerosol has a CCN activity higher than pure $(NH_4)_2SO_4$. This increase in CCN activity is due to the surface tension

depression observed at the lower organic fractions which allows the droplet activation at lower supersaturations. The same behavior was observed for all mixtures.

Comparison of CCN activity (activation curves) are presented in Figs. 7a and b for pure organic aqueous solution and their mixture with $(NH_4)_2SO_4$. The observed CCN activity was not consistent with solubility reported in Table 2; in fact all compounds studied behaved as if they were completely soluble, possibly because of curvature-enhanced solubility (Padró and Nenes, 2007[2]). As the measurements suggest that most compounds are not strong surfactants (Fig. 4), CCN activity correlates with the number of moles at the point of activation, i.e., the effective van't Hoff factor (the moles of ions released per mol of solute) over the molar volume. For example, phthalic acid is better CCN than fructose; the two have comparable molar volumes (Table 2) but the carboxyl groups in phthalic acid dissociate substantially (low pKa, i.e. van't Hoff factor >1), while fructose does not dissociate at all (i.e. van't Hoff factor = 1). Using this approach, one can rank the compounds in terms of decreasing CCN activity as follows: ammonium sulfate, phthalic acid, malonic acid, succinic acid, leucine, azelaic acid, and fructose. Our measurements support this ranking.

4.3 Evaluation of inferred molar volumes

Köhler theory analysis requires knowledge of the parameters α, β (Tables 3 and 4), and ω (Table 5), which are introduced into Eq. (9). The calculated $\left(\frac{M_j}{\rho_j}\right)$ as well as its error with respect to expected values are shown in Table 5. Predicted molar volume of each organic was closest to literature values when the organic mass fraction is 50% and above; under such conditions, the average error in inferred molar volume was found to be 18%. For pure organic CCN, the solute may not completely dissolve at the point of activation, therefore the solute molar volume can be largely overestimated (Table 5). Addition of some deliquescent material (ammonium sulfate) enhances the

[2]Padró, L. T. and Nenes, A.: Cloud droplet activation: solubility revisited, Atmos. Chem. Phys. Discuss., in review, 2007.

amount of water in the CCN and facilitates complete dissolution of the organic fraction (the solubility of which can be further enhanced from curvature-enhanced solubility, Padró and Nenes, 2007[2]). As a result, the inferred molar volume error decreases as s_c more closely scales with $d^{-3/2}$. When the organic fraction becomes low (<50%), the CCN at the point of activation becomes concentrated in ammonium sulfate and the organic may "salt out" (i.e., precipitate out of solution). This affects the solution surface tension and number of dissolved moles, which eventually increases the error in molar volume (Table 5). Phthalic acid is in less error compared to leucine and azelaic acid (despite the "bulk" solubility of the former is lower than the latter), possibly because particle curvature may eventually enhance its solubility to the point of complete dissolution. Overall, the assumption of complete solubility used in KTA seems to work well, particularly for cases where organics are mixed with some sulfate.

Estimating molar volume uncertainty requires computing its sensitivity with respect to σ, ϖ , υ_j and the estimated uncertainty in those parameters (Table 6). Of the three parameters, ϖ and υ_j were found to introduce the greatest uncertainty; while the uncertainty in σ is rather small. The greater uncertainty (~55%) for all the compounds arises from the van't Hoff factor (dissociation in water). The uncertainty in this parameter is high since in our study it was assumed that υ_j=1 when in reality it is larger since most of the dicarboxylic acids we studied dissociate (pKa<3). Error estimates increase dramatically as the organic fraction decreases, since the sensitivities, Φ_x, depend inversely on the organic mass fraction (Table 1).

From our assessment of KTA, the new method applies best for relatively high organic mass fractions but with some deliquescent material to insure sufficient water uptake for complete dissolution of constituents. It is suggested that the method should not be used for low organic fraction aerosols because: *i*) salting out effects can become important and *ii)* the sensitivities scale with ε_j^{-1} and uncertainties are magnified substantially for volume fractions below 20%. The uncertainty estimated from Eq. (10) (Table 6) is usually larger than the actual molar volume (Table 5), which suggests that Eq. (10) can be used as an upper limit estimate.

5 Conclusions

This study presents a new method, Köhler Theory Analysis (KTA), to infer the molar volume, solubility, and surfactant characteristics of water soluble atmospheric organic matter. This is done by combining Köhler theory with measurements of surface tension, chemical composition, and CCN activity. In addition to presenting KTA, we evaluate the method by comparing inferred molar volumes to their expected values for particles composed of six organics (azelaic acid, malonic acid, phthalic acid, succinic acid, leucine, and fructose) in pure form or mixed with $(NH_4)_2SO_4$. CCN activation experiments were done at 0.2%, 0.4%, 0.6%, and 1.2% supersaturation.

Köhler theory analysis was found to predict the molar volume to within 18% of expected value when the organic mass fraction ranges between 50 and 100%. The estimated molar volume error was found to be larger than reality. KTA is a powerful tool for characterizing the droplet formation potential of ambient water soluble organic carbon (WSOC) and provide constraints needed for physically-based assessments of the aerosol indirect effect.

Acknowledgements. This research was supported by a NSF CAREER Award, NASA Headquarters under the Earth System Science Fellowship Grant and another NASA Proposal (NNG04GE16G).

References

CRC handbook of Chemistry and Physics, CRC Press, New York, 2002.

Abbatt, J. P. D., Broekhuizen, K., and Kumal, P. P.: Cloud condensation nucleus activity of internally mixed ammonium sulfate/organic acid aerosol particles, Atmos. Environ., 39(26), 4767–4778, 2005.

Albrecht, B. A.: Aerosols, cloud microphysics, and fractional cloudiness, Science, 245, 1227–1230, 1989.

Broekhuizen, K., Chang, R. Y.-W., Leaitch, W. R., Li, S.-M., and Abbatt, J. P. D.: Closure between the measured and modeled cloud condensation nuclei (CCN) using size-resolved

aerosol compositions in downtown Toronto, Atmos. Chem. Phys. Discuss., 6, 2513–2524, 2006, http://www.atmos-chem-phys-discuss.net/6/2513/2006/.
Cruz, C. N. and Pandis, S. N.: A study of the ability of pure secondary organic aerosol to act as cloud condensation nuclei, Atmos. Environ., 31(15), 2205–2214, 1997.
Decesari, S., Facchini, M. C., Fuzzi, S., and Tagliavini, E.: Characterization of water soluble organic compounds in atmospheric aerosol: A new approach, J. Geophys. Res.-A., 105(D1), 1481–1489, 2000.
Facchini, M. C., Decesari, S., Mircea, M., Fuzzi, S., and Loglio, G.: Surface tension of atmospheric wet aerosol and cloud/fog droplets in relation to their organic carbon content and chemical composition, Atmos. Environ., 34(28), 4853–4857, 2000.
Facchini, M. C., Fuzzi, S., Zappoli, S., Andracchio, A., Gelencser, A., Kiss, G., Krivacsy, Z., Meszaros, E., Hansson, H. C., Alsberg, T., and Zebuhr, Y.: Partitioning of the organic aerosol component between fog droplets and interstitial air, J. Geophys. Res.-A., 104(D21), 26 821–26 832, 1999a.
Facchini, M. C., Mircea, M., Fuzzi, S., and Charlson, R. J.: Cloud albedo enhancement by surface-active organic solutes in growing droplets, Nature, 401(6750), 257–259, 1999b.
Feingold, G. and Chuang, P. Y.: Analysis of the influence of film-forming compounds on droplet growth: Implications for cloud microphysical processes and climate, J. Atmos. Sci., 59(12), 2006–2018, 2002.
Giebl, H., Berner, A., Reischl, G., Puxbaum, H., Kasper-Giebl, A., and Hitzenberger, R.: CCN activation of oxalic and malonic acid test aerosols with the University of Vienna cloud condensation nuclei counter, J. Aerosol Sci., 33(12), 1623–1634, 2002.
Hartz, K. E. H., Tischuk, J. E., Chan, M. N., Chan, C. K., Donahue, N. M., and Pandis, S. N.: Cloud condensation nuclei activation of limited solubility organic aerosol, Atmos. Environ., 40(4), 605–617, 2006.
IPCC, Climate Change (2001): The Scientific Basis, Cambridge University Press. United Kingdom, 2001.
Kanakidou, M., Seinfeld, J. H., Pandis, S. N., Barnes, I., Dentener, F. J., Facchini, M. C., Van Dingenen, R., Ervens, B., Nenes, A., Nielsen, C. J., Swietlicki, E., Putaud, J. P., Balkanski, Y., Fuzzi, S., Horth, J., Moortgat, G. K., Winterhalter, R., Myhre, C. E. L., Tsigaridis, K., Vignati, E., Stephanou, E. G., and Wilson, J.: Organic aerosol and global climate modelling: a review, Atmos. Chem. Phys., 5, 1053–1123, 2005,

http://www.atmos-chem-phys.net/5/1053/2005/.
Kiss, G., Tombacz, E., and Hansson, H. C.: Surface tension effects of humic-like substances in the aqueous extract of tropospheric fine aerosol, J. Atmos. Chem., 50(3), 279–294, 2005.
Kohler, H.: The nucleus in and the growth of hygroscopic droplets, Transactions of the Faraday Society, 32(2), 1152–1161, 1936.
Kumar, P. P., Broekhuizen, K., and Abbatt, J. P. D.: Organic acids as cloud condensation nuclei: Laboratory studies of highly soluble and insoluble species, Atmos. Chem. Phys., 3, 509–520, 2003,
http://www.atmos-chem-phys.net/3/509/2003/.
Langmuir, I.: The constitution and fundamental properties of solids and liquids. II. Liquids., J. Am. Chem. Soc., 39, 1848–1906, 1917.
Nenes, A., Charlson, R. J., Facchini, M. C., Kulmala, M., Laaksonen, A., and Seinfeld, J. H.: Can chemical effects on cloud droplet number rival the first indirect effect?, Geophys. Res. Lett., 29(17), 1848, doi:10.1029/2002GL015295, 2002.
Raymond, T. M. and Pandis, S. N.: Cloud activation of single-component organic aerosol particles, J. Geophys. Res.-A., 107(D24), 4787, doi:10.1029/2002JD002159, 2002.
Roberts, G. C. and Nenes, A.: A continuous-flow streamwise thermal-gradient CCN chamber for atmospheric measurements, Aerosol Sci. Technol., 39(3), 206–211, 2005.
Rosenoern, T., Kiss, G., and Bilde, M.: Cloud droplet activation of saccharides and levoglucosan particles, Atmos. Environ., 40, 1794–1802, 2006.
Saxena, P. and Hildemann, L. M.: Water soluble organics in atmospheric particles: A critical review of the literature and application of thermodynamics to identify candidate compounds, J. Atmos. Chem., 24(1), 57–109, 1996.
Seinfeld, J. H. and Pandis, S.: Atmospheric Chemistry and Physics, John Wiley. New York, 1997.
Shulman, M. L., Jacobson, M. C., Carlson, R. J., Synovec, R. E., and Young, T. E.: Dissolution behavior and surface tension effects of organic compounds in nucleating cloud droplets, Geophys. Res. Lett., 23(3), 277–280, 1996.
Solomons, G. and Fryhle, C.: Organic Chemistry, John Wiley & Sons, Inc. New York, 2000.
Spelt, J. K. and Li, D.: Applied Surface Thermodynamics, MARCEL DEKKER, INC. New York, 1996.
Sullivan, A. P. and Weber, R. J.: Chemical characterization of the ambient organic aerosol soluble in water: 1. Isolation of hydrophobic and hydrophilic fractions with a XAD-8 resin, J.

Geophys. Res.-A., 111(D5), D05314, doi:10.1029/2005JD006485, 2006a.
Sullivan, A. P. and Weber, R. J.: Chemical characterization of the ambient organic aerosol soluble in water: 2. Isolation of acid, neutral, and basic fractions by modified size-exclusion chromatography, J. Geophys. Res.-A., 111(D5), D05315, doi:10.1029/2005JD006486, 2006b.
Twomey, S.: Minimum size of particle for nucleation in clouds, J. Atmos. Sci., 34, 1832–1835, 1977.
Yaws, C. L.: Yaw's handbook of thermodynamic and physical properties of chemical compounds, Knovel. New York, 2003.
Zappoli, S., Andracchio, A., Fuzzi, S., Facchini, M. C., Gelencser, A., Kiss, G., Krivacsy, Z., Molnar, A., Meszaros, E., Hansson, H. C., Rosman, K., and Zebuhr, Y.: Inorganic, organic and macromolecular components of fine aerosol in different areas of Europe in relation to their water solubility, Atmos. Environ., 33(17), 2733–2743, 1999.

Table 1. Formulas used for computing the sensitivity of molar volume to σ, ω, and υ_j.

Property	Sensitivity, $\Phi_x = \frac{\partial}{\partial x}\left(\frac{M_j}{\rho_j}\right)$
σ	$\Phi_\sigma = \frac{768}{27}\left(\frac{M_w}{\rho_w}\right)^2\left(\frac{1}{RT}\right)^3\left(\frac{M_j}{\rho_j}\right)^2\frac{\sigma^2}{\varepsilon_j\upsilon_j\omega^2}$
ω	$\Phi_\omega = -\frac{512}{27}\left(\frac{M_w}{\rho_w}\right)^2\left(\frac{1}{RT}\right)^3\left(\frac{M_j}{\rho_j}\right)^2\frac{\sigma^3}{\varepsilon_j\upsilon_j\omega^3}$
υ_j	$\Phi_\upsilon = -\frac{256}{27}\left(\frac{M_w}{\rho_w}\right)^2\left(\frac{1}{RT}\right)^3\frac{\sigma^3}{\varepsilon_j\upsilon_j^2\omega^2} + \sum_{i\neq j}\frac{\left(\frac{\rho_j}{M_i}\right)\varepsilon_i\upsilon_i}{\varepsilon_j\upsilon_j^2}$

Table 2. Properties of compounds considered in this study. Organics are sorted in order of decreasing solubility.

Compound Name	Chemical Formula	Molar Mass ($g\,mol^{-1}$)	Density ($g\,cm^{-3}$)	Solubility (g/100g H_2O)	Molar Volume ($cm^3\ mol^{-1}$)	pKa[g]
Fructose	$C_6H_{12}O_6$	180.16	1.600[c]	407.4[c]	113	N/A
Malonic Acid	$C_3H_4O_4$	104.06	1.619[a]	154[d]	64	2.9 (5.7)
Succinic Acid	$C_4H_6O_4$	118.09	1.566[b]	8.76[b]	75	4.2 (5.6)
Leucine	$C_6H_{13}NO_2$	131.17	1.293[e]	2.3[e]	101	2.4 (5.98) (acid) 9.60 (amine)
Azelaic Acid	$C_9H_{16}O_4$	188.22	1.225[f]	0.2447[f]	154	N/A
Phthalic Acid	$C_8H_6O_4$	166.13	1.593[b]	0.1415[f]	104	2.9 (5.4)
Ammonium Sulfate	$(NH_4)_2SO_4$	132.14	1.77[d]	41.22[d]	74.66	

[a] Abbat et al. (2005).
[b] Hartz et al. (2006).
[c] Rosenørn et al. (2006).
[d] Material Safety Data Sheet.
[e] CRC Handbook (2002).
[f] Yaws' Handbook (2003).
[g] Solomons and Fryhle (2000).

Table 3. Szyskowski-Langmuir constants (298 K) for computing the surface tension of aqueous organic solutions. The same parameters apply for pure organic solutions and mixtures with $(NH_4)_2SO_4$ (up to 10% salt mol fraction). C_{max} is the maximum concentration of organic used in the measurements.

Compound	$\alpha \times 10^1$ (mN m^{-1}K^{-1})	$\beta \times 10^5$ (ppm^{-1})	$C_{max} \times 10^{-3}$ (ppm)
Fructose	1.900	0.0709	180
Malonic Acid	0.434	1.0000	1040
Succinic Acid	0.652	1.3400	59
Leucine	1.950	0.5700	13
Azelaic Acid	0.484	9.4900	1.9
Phthalic Acid	1.930	0.9170	0.831

Table 4. Szyskowski-Langmuir constants (298 K) for computing the surface tension of aqueous organic solutions mixed with $(NH_4)_2SO_4$ for larger than 10% salt mole fraction.

Compound	Organic Mole Fraction (%)	$\alpha \times 10^1$ (mN $m^{-1}K^{-1}$)	$\beta \times 10^5$ (ppm^{-1})
Malonic Acid	50	3.5968	0.957
	10	0.0708	234.6
	1	0.1254	141.3
Succinic Acid	50	0.0185	1000
	10	1.8000	2.760
	1	3.4800	2.200
Azelaic Acid	50	0.2045	454.4
	10	0.6953	86.9
	1	9.7600	7.440

Table 5. Results of Köhler theory analysis for the compounds and mixtures considered in this study. Organics are arranged in order of decreasing solubility.

Compound (Molar Volume)	Organic Mole Fraction (%)	$\omega \times 10^{14}$ ($m^{-2/3}$)	Inferred Molar Volume ($cm^3\ mol^{-1}$)	Molar Volume Error (%)
Fructose	100	8.478	112.868	0.2
($113\ cm^3\ mol^{-1}$)	99	8.527	115.207	2
	95	8.075	111.447	1
	90	7.587	106.600	5
Malonic Acid	100	6.473	66.150	3
($64\ cm^3\ mol^{-1}$)	99	6.398	65.089	1
	95	6.195	63.531	1
	90	5.944	62.145	3
	50	4.5878	68.328	6
	10	3.9651	3.082	95
	1	3.9043	0.016	100
Succinic Acid	100	6.839	89.368	19
($75\ cm^3\ mol^{-1}$)	99	6.777	88.680	18
	95	6.550	81.394	8
	90	6.227	76.909	2
	50	4.7531	58.130	23
	10	4.0245	7.313	90
	1	3.8638	0.099	100
Leucine	100	7.810	139.106	37
($101\ cm^3\ mol^{-1}$)	99	7.960	183.440	81
	95	7.438	125.739	24
	90	7.054	113.670	12
Azelaic Acid	100	8.146	281.794	83
($154\ cm^3\ mol^{-1}$)	99	7.870	190.044	23
	95	7.062	135.549	12
	90	6.804	131.878	14
	50	3.9864	212.967	38
	10	2.4622	161.931	5
	1	4.0991	691.836	349
Phthalic Acid	100	5.790	90.024	14
($104\ cm^3\ mol^{-1}$)	99	5.600	82.449	21
	95	5.620	89.298	14
	90	5.630	107.624	3

Table 6. Molar volume uncertainty analysis and total uncertainty as percent of molar volume for the compounds and mixtures considered in this study.

Compound	Organic Mole Fraction (%)	Uncertainty to σ (cm^3 mol^{-1})	Uncertainty to ω (cm^3 mol^{-1})	Uncertainty to υ_{org} (cm^3 mol^{-1})	Total Uncertainty (cm^3 mol^{-1})	Total Uncertainty (%)
Fructose	100	0.192	16.166	22.453	38.811	34.3
	99	0.250	16.227	22.537	39.014	34.5
	95	0.246	18.789	26.095	45.130	40.0
	90	0.241	22.588	31.372	54.200	48.0
Malonic	100	0.064	6.641	9.224	15.802	24.7
Acid	99	0.058	6.909	9.596	16.448	25.7
	95	0.037	7.764	10.783	18.510	28.9
	90	0.064	8.937	12.412	21.285	33.3
	50	0.222	14.479	31.807	46.064	72.0
	10	0.821	215.477	169.300	383.956	599.9
	1	14.756	2620.228	2600.989	5206.452	8135.1
Succinic	100	0.103	8.046	12.572	20.515	27.4
Acid	99	0.106	8.265	12.915	21.074	28.1
	95	0.126	10.043	15.692	25.608	34.1
	90	0.170	12.424	19.413	31.668	42.2
	50	0.364	52.018	59.111	110.765	147.7
	10	2.569	124.850	346.807	469.089	625.5
	1	28.494	2787.770	3871.907	6631.177	8841.6
Leucine	100	0.138	8.529	11.846	20.237	20.0
	99	0.093	6.337	8.801	15.044	14.9
	95	0.130	11.045	15.341	26.257	26.0
	90	0.224	14.998	20.830	35.604	35.3
Azelaic	100	0.227	13.847	18.219	31.839	20.7
Acid	99	0.258	18.859	24.814	43.414	28.2
	95	0.479	27.903	36.714	64.138	41.6
	90	0.453	35.492	46.700	81.738	53.1
	50	0.951	50.995	106.240	156.284	101.5
	10	7.624	490.647	721.541	1204.567	782.2
	1	70.198	13 308.622	12 322.813	25 561.27	16 598.2
Phthalic	100	0.436	40.802	56.669	97.907	94.1
Acid	99	0.427	45.036	62.549	108.007	103.9
	95	0.435	46.667	64.813	111.913	107.6
	90	0.471	51.794	71.936	124.201	119.4

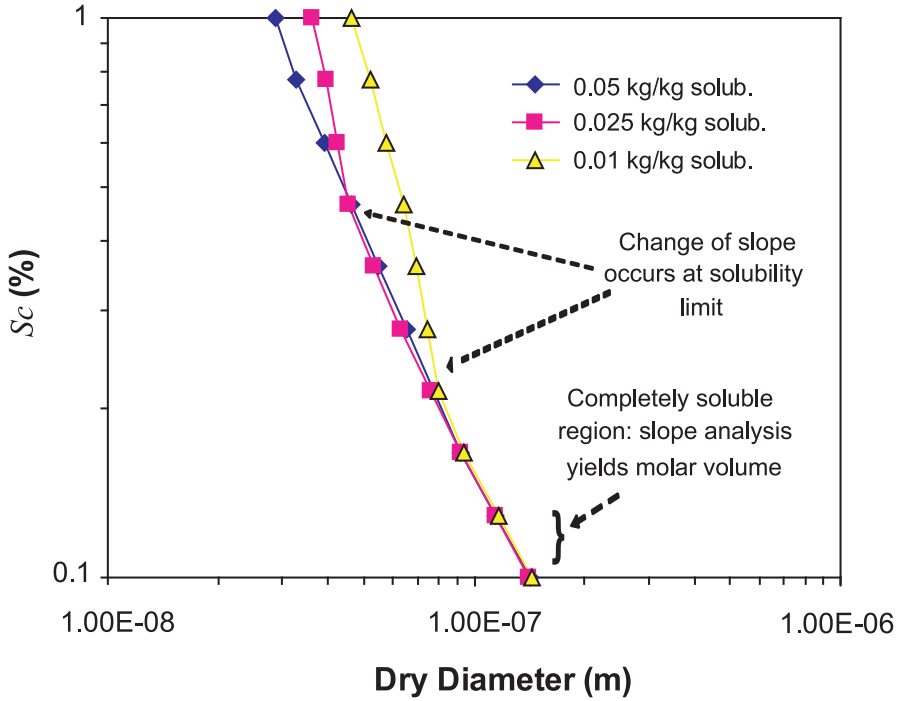

Fig. 1. Example on how CCN activation experiments can be used to infer the solubility of compounds.

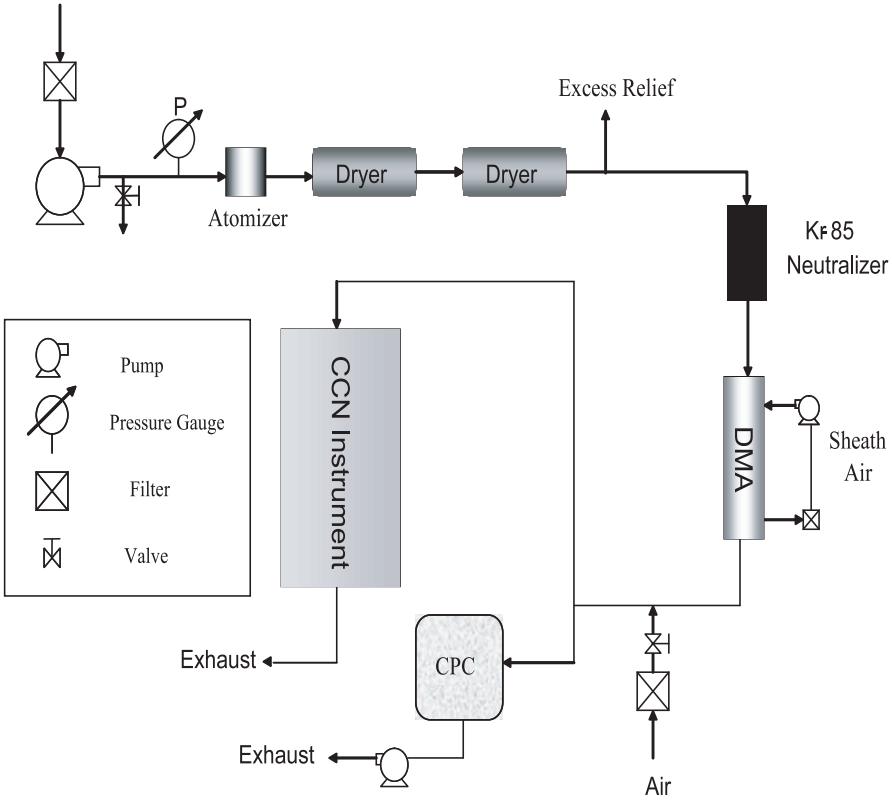

Fig. 2. Experimental setup used to measure CCN activity.

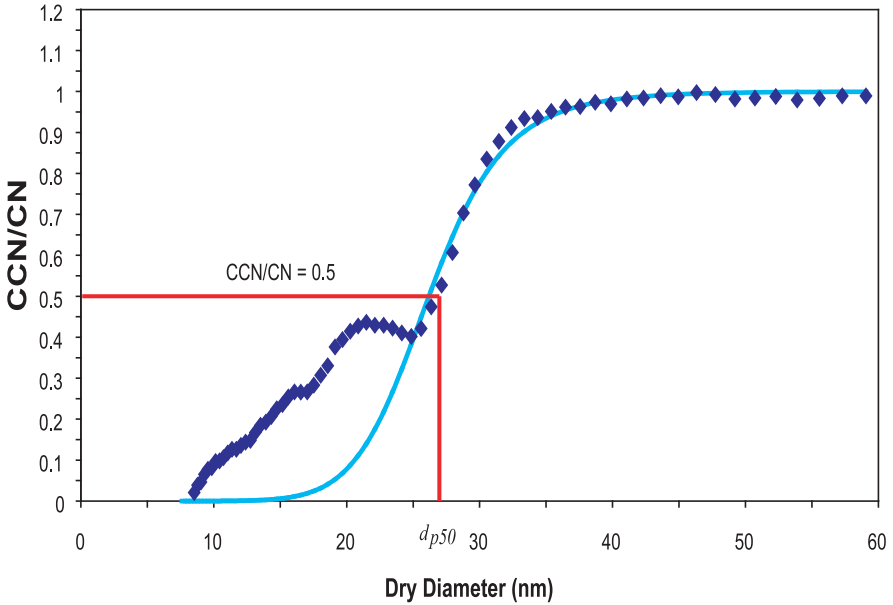

Fig. 3. Example of procedure used to determine d_{p50}. Shown are data obtained at 1.2% supersaturation of CCN/CN data for 50% malonic acid with its sigmoidal fit (light blue line). d_{p50} is the dry diameter for which CCN/CN=0.5.

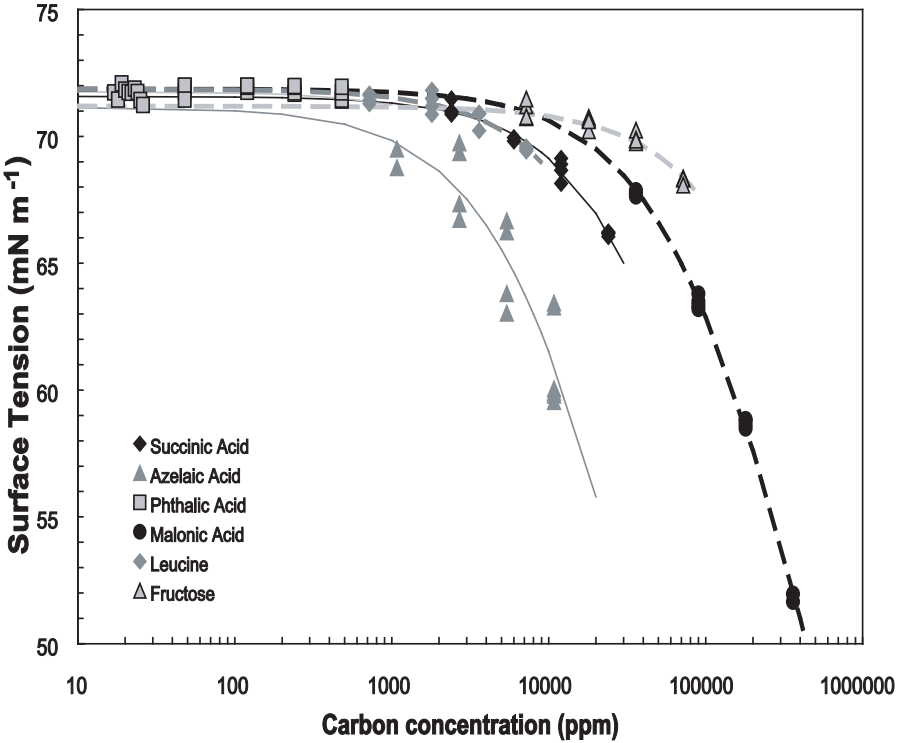

Fig. 4. Surface tension as a function of concentration of mixed organic/inorganic aqueous solutions. Shown are succinic acid (black diamond), azelaic acid (grey triangle), phthalic acid (outlined grey square), malonic acid (black circle), leucine (grey diamond), and fructose (outlined grey triangle). The lines correspond to the Szyskowski-Langmuir fit for each organic.

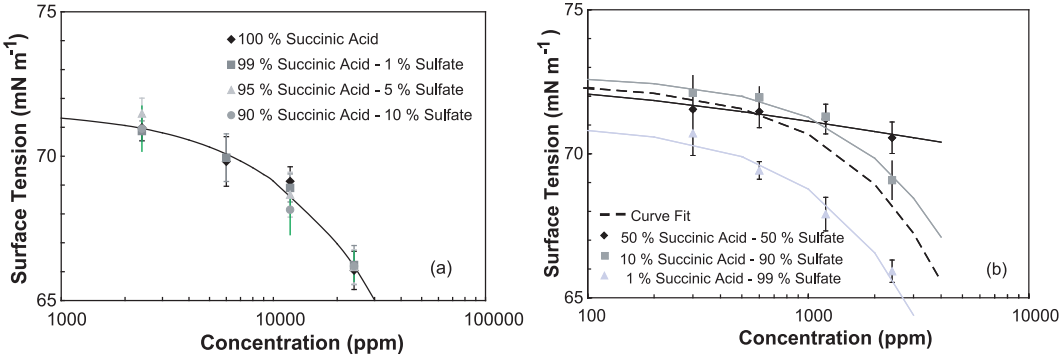

Fig. 5. (a) Surface tension as a function of concentration for pure succinic acid (black diamond) and mixtures with $(NH_4)_2SO_4$ for 99% (grey square), 95% (grey triangle), and 90% (grey circle) succinic acid (mol fraction). The solid black line corresponds to the Szyskowki-Langmuir fit for all high organic fraction mixtures. **(b)** Surface tension depression as a function of concentration for $(NH_4)_2SO_4$ – succinic acid mixtures for 50% (black diamond), 10% (grey square), and 1% (grey triangle) succinic acid (mol fraction). The solid lines correspond to the Szyskowski-Langmuir fit for each mixture: 50% (black line), 10% (dark grey line), and 1% (light grey line). The dashed black line corresponds to the Szyskowski-Langmuir fit for all three low organic fraction mixtures.

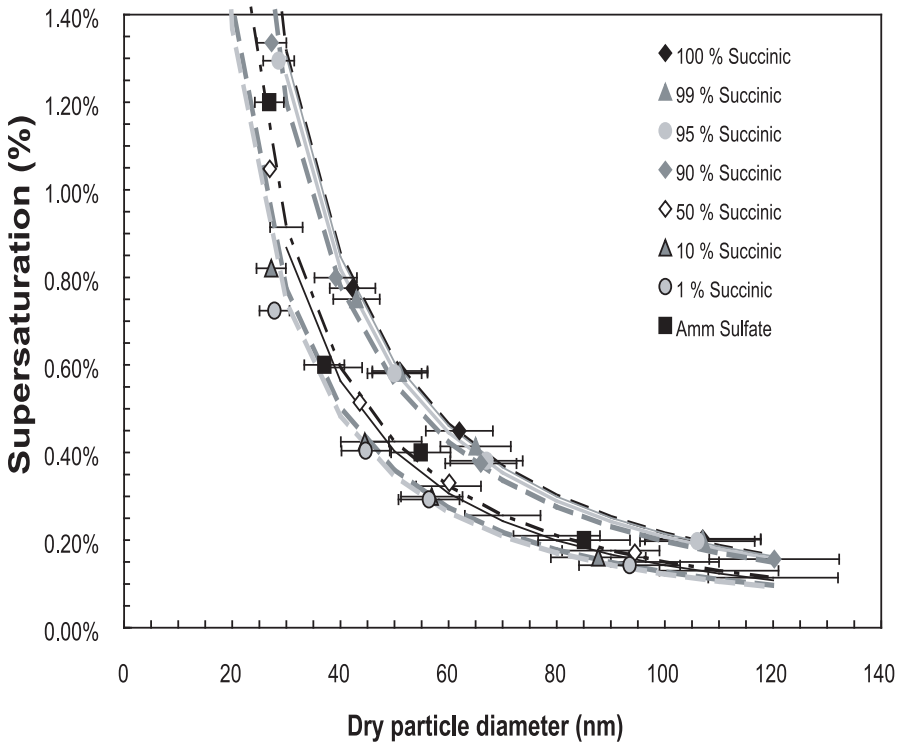

Fig. 6. Activation curve for pure succinic acid (black diamond) and mixtures with $(NH_4)_2SO_4$ consisting of 99% (grey triangle), 95% (grey circle), 90% (grey diamond), 50% (open diamond), 10% (outlined grey triangle), and 1% (outlined grey circle) molar fraction of succinic acid. Activation curve for $(NH_4)_2SO_4$ (black square) is also plotted for comparison. The solid and dash lines (100% (black dash line), 99% (dark grey line), 95% (light grey line), 90% (dark grey dashed line), 50% (black dash dot line), 10% (dashed dark grey), 1% (dashed light grey) and $(NH_4)_2SO_4$ (black line)) indicates a power fit to the data.

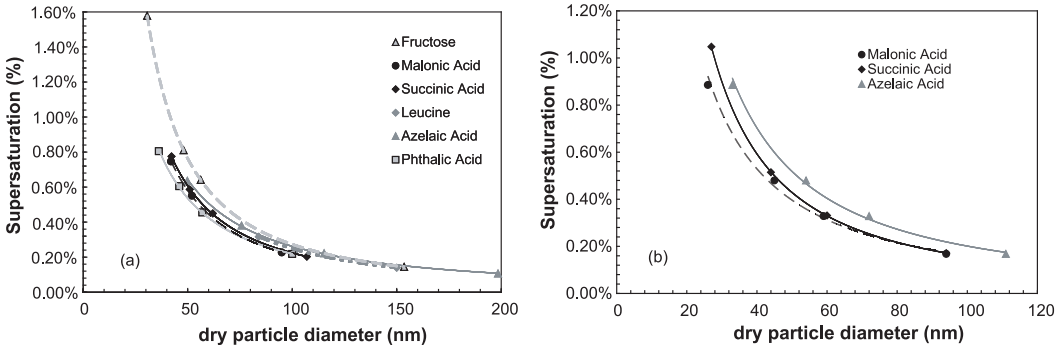

Fig. 7. (a) Activation curves for pure organic components: succinic acid (black diamond), azelaic acid (grey triangle), phthalic acid (outlined grey square), malonic acid (black circle), leucine (grey diamond), and fructose (outlined grey triangle). The lines correspond to a power law fit to the activation data. **(b)** Activation curves for 50% organic fraction mixtures with $(NH_4)_2SO_4$: azelaic acid (grey triangle), phthalic acid (outlined grey square), and malonic acid. The lines correspond to a power law fit to the activation data.